ENGINEER - Vol. LVI, No. 02, pp. [51-64], 2023

DOI: https://doi.org/10.4038/engineer.v56i2.7576

# Enhancement of the Lateral Performance of RC Columns Using Steel Jacketing: A Numerical Approach

**Y.G.P. Erange, M. Jenothan, J.A.S.C. Jayasinghe, C.S. Bandara and A.J. Dammika**

**Abstract:** Steel jacketing has become an attractive strengthening technique for reinforced concrete (RC) columns due to ease of construction and less space requirement. The steel cage consists of angle sections placed at corners and held together by battens at intervals along the RC column height. A numerical investigation of the effective use of steel jackets as a strengthening technique in RC columns is presented in this paper. First, the finite element models of the strengthened column were developed and validated using past experimental data. Then, with the validated model, six sets of steel jacket sections with modified cross-sections such as batten spacing, batten thickness, batten width, end batten width, L angle thickness and steel jacket height were tested under constant axial and lateral loading to understand the effectiveness of steel jackets as the strengthening technique. AnunstrengthenRC column were also analysed to compare the performance of a similar column strengthened by steel jackets with modified parameters. It was shown that strengthening RC columns with steel jackets was effective in enhancing the lateral performance of the columns and resulted in a more stable load-displacement curve with lower strength degradations as compared with the un-strengthened ones. Additionally, it was found that the most effective method to increase the lateral strength and ductility is increasing the L angle thickness. On the other hand, increasing the steel jacket height also increases the lateral performance, however, it was identified that increasing the jacket height is effective only up to 1/3rd of the RC column height. Finally, the obtained results for each parameter were compared to study the behaviour of each component of the steel jacket towards lateral strength and ductility improvements.

**Keywords**: Concrete damage plasticity model, Lateral performance, Non-linear finite element analysis, RC column, Steel jacket, Strengthening technique

## 1. Introduction

Strengthening of existing structures has evolved as a critical construction activity in response to revised design rules and strength requirements, as well as environmental deterioration over time [1]. Existing reinforced concrete structures built before the earthquake-resistant design techniques cannot provide appropriate ductility during earthquakes[2]. In particular, brittle columns without proper transverse reinforcement may lead to the total collapse of this type of construction due to insufficient deformation capacity[3]. As a result, adequate reinforcements are necessary to achieve strength requirements and extend the service life of RC columns. Construction flaws are another significant problem with RC columns, and the majority of these damages have been demonstrated in RC columns with insufficient axial/shear load capacity because of inadequate longitudinal/transversal reinforcement and dimensions, 90-degree hooks for stirrups at both ends of columns, inadequate detailing in beam-column joint regions, strong-

*Eng. Y.G.P. Erange, AMIE(SL), B.Sc. Eng. (Hons) (Peradeniya), M.Eng. (Reading), Regional Engineer, Sri Lanka Land Development Corporation.*
*Email:era.erange@gmail.com*
*http://orcid.org/0000-0002-6739-4767*
***Eng. M. Jenothan**, AMIE(SL), B.Sc. Eng. (Hons) (Peradeniya), M.Eng., Temporary Instructor, University of Peradeniya.*
*Email:makeswaranjenothan@eng.pdn.ac.lk*
*http://orcid.org/0000-0001-5112-1548*
***Eng. (Dr.) J.A.S.C. Jayasinghe,** AMIE(SL) B.Sc. Eng. (Hons), MEng. (AIT), PhD.(Tokyo), Senior Lecturer, Department of Civil Engineering, Faculty of Engineering, University of Peradeniya.*
*Email:supunj@eng.pdn.ac.lk*
*http://orcid.org/0000-0003-1054-9358*
***Eng. (Dr.) C.S. Bandara,** C.Eng., MIE(SL), B.Sc. Eng. (Peradeniya), M.Sc. Eng. (Peradeniya), PhD. (Peradeniya), Senior Lecturer, Department of Civil Engineering, Faculty of Engineering, University of Peradeniya.*
*Email:csbandara@eng.pdn.ac.lk*
*http://orcid.org/0000-0003-4141-8983*
***Eng. (Dr.) A.J. Dammika**, AMIE(SL), BSc. Eng. (Hons) (Peradeniya), MEng. (AIT), Ph.D. (Saitama), Senior Lecturer, Department of Civil Engineering, University of Peradeniya.*
*Email:dammikaaj@eng.pdn.ac.lk*
*http://orcid.org/0000-0002-2587-3743*

beam and weak-columns, soft stories, weak stories, and unsatisfactory construction [4,5].

However, external strengthening of RC columns can solve most of the abovementioned issues, and it is preferable if the procedure is less disruptive, rapid, and inexpensive. Traditional RC structure strengthening procedures include the application of an exterior layer of a metallic plate, textile fibre sheet, wire mesh, post-tensioning, concrete or steel jacketing, and epoxy injection [6–12].

Since there are numerous strategies for strengthening reinforced concrete (RC) columns as a viable rehabilitation technique to upgrade RC columns, externally bonded fibre-reinforced polymers (FRP) have been the subject of numerous studies [3,6,8,9,13]. It has been demonstrated that although the FRP system improved RC column's ductility and energy absorption capacity, there was no substantial increase in strength [9]. Composite jackets are approximately one-fourth the weight of steel. It is simple to apply in confined areas, eliminates the need for heavy surface preparation, decreases labour costs, and provides excellent ductility. However, the worst characteristics identified over the composite jacketing are its susceptibility to fire and the composite material's linearly elastic behaviour, which leads to member failure without yielding or plastic deformation resulting in poor ductility [14].

The installation of a thin layer of reinforced concrete around an existing RC column is referred to as RC jacketing [14]. A suitable number of anchor bars/shear keys and adhesive materials are used to ensure a satisfactory connection between the old and new concrete surfaces. It is expected that the confinement enhancement will be simple since the transverse reinforcement may be attached to the exterior of the longitudinal bars at any necessary spacing. However, confinement by RC jacketing is less effective on rectangular or square cross-sections than on circular cross-sections. It is simple to set up, and improves ductility, shear strength, and load-bearing capability. In contrast, one of the most significant disadvantages of RC jacketing is the inability to enlarge sections [15].

Steel jacketing is one such approach, which comprises four steel angles at the RC column's corners and welded steel plates at a few locations along its length or full external steel plate jacketing (see Figure 1). This technique is a simple, quick, low-cost method for increasing structural elements' carrying capacity, lateral strength, ductility, and shear capacity [16–18].

During the past few decades, occurrences of earthquakes across the world kept increasing. So, it is necessary to study the improvements to the seismic behaviour of the structures by increasing lateral strength and ductility. Most researchers have studied only the axial capacity improvement of the RC column using various strengthening techniques. However, considerable research has been conducted on FRP during the last two decades. There is less research on steel jacketing than the other two methods, and studies on the lateral strengthening of steel jacketed columns are even lesser [12]. Steel jacketing techniques have several advantages over FRP, such as being less interruptive, less time-consuming, less expensive, and minimum loss of floor area. Therefore, understanding the lateral performance of the RC column with the steel jacketing technique is essential. Furthermore, studying the behaviour of each parameter (see Figure 1) of the steel jacket system to enhance its lateral performance indices is the crucial element that improves the lateral performance of the strengthened column.

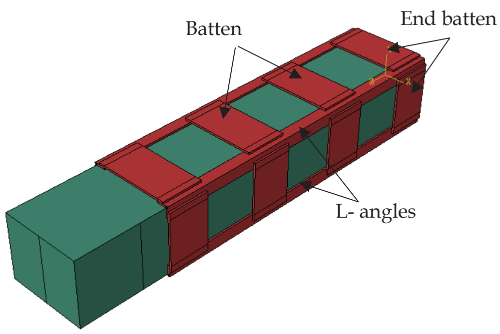


**Figure 1 - Typical Steel Jacketing to RC Column**

Therefore, the objective of this study is to investigate the lateral performance of reinforced concrete (RC) columns strengthened with a steel jacketing technique that uses four steel angles welded with horizontal steel plates. Further, this study aims to understand the behaviour of each parameter of the steel jacket system to enhance the lateral performance indices of the strengthened column, including improvements in lateral strength, yield strength, and ductility. This will contribute to the development of more effective and efficient seismic strengthening techniques for RC columns.

The parameters called lateral performance indices (see Figure 2) were used to compare and evaluate the lateral performance enhancement due to the strengthening technique used in this study. The lateral performance indices are specific places on the hysteresis envelope curve where the engineer may evaluate the enhancement in the performance of RC column due to the strengthening technique. As mentioned in Figure 2, H and δ denote the horizontal load and corresponding displacement at the RC column top, respectively. The points $(\delta_y, H_y)$ and $(\delta_m, H_m)$ represent the yield point and the point at which the bearing capacity reaches to its peak value.

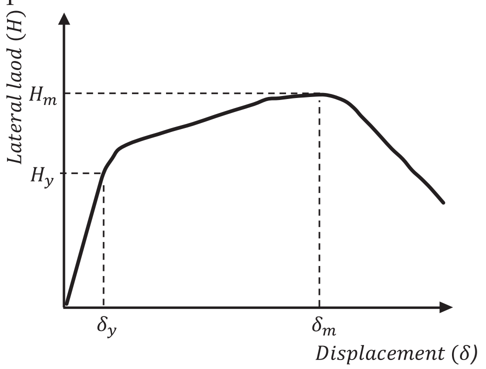


**Figure 2 - Hysteresis Envelope Curve Strengthen RC Column Under Lateral Cyclic Loading [19]**

First, the developed finite element model of the test specimen was validated using past experimental data from the literature [7]. Next, the validated model was used to perform the parametric study to identify the seismic behaviour of each element of the steel jacketing system, such as jacket height, batten thickness and width, batten spacing and L angle thickness. Then, the results were compared with the standard strengthened and unstrengthen models to compare the effectiveness of each element modification of the steel jacket. Finally, the results were discussed, and recommendations were given to effectively enhance the RC column's performance using steel jackets.

## 2. Numerical Analysis

In the past, research on the ultimate strength and ductility capacity of strengthened RC columns was primarily limited to experiments. The experimental approaches, however, fall well short of covering structural parameters. With the rapid growth of computer capability and accurate constitutive law, numerical approaches for determining the ultimate strength and ductility of strengthened RC columns are gaining popularity. However, various analytical methods exist to perform a non-linear analysis, such as the finite element (FE), plastic hinge and empirical methods. However, the FE method is the most popular and accurate since it can represent both material and geometric non-linearities [20]. Furthermore, several failure modes can be identified using the FE model, and various physical events can be tested within a standard model. Another advantage of the FE approach is that it can handle simultaneous calculation and visual representation of various physical parameters such as stress, deflection and temperature. Therefore, it enables the designer to analyse the performance and possible modifications rapidly.

### 2.1. Material Modeling

In this study, ABAQUS FE software used, which has a vast number of the material model library which is capable of simulating tension softening, tension stiffening of material with boundary and geometry non-linearity of the model. Further, it has the features such as visualising the crack pattern, crack propagation of solid elements [20,21]. The elastic behaviour of concrete is modelled using simple linear elasticity with Young's modulus and Poison's ratio. However, different models are adopted to represent the failure envelope for plastic states, where deformations become irreversible. There are mainly four models: smeared crack model, brittle crack model, concrete damage plasticity (CDP) model and Mohr-Coulomb failure criterion method.

The smeared crack model method spreads the crack formation over the whole element. Therefore, it is challenging to predict localised failure. However, this method precisely predicts concrete load deflection and local strain behaviour [22]. The brittle crack model can model concrete in all types of structures, but it only considers the elastic behaviour. As a result, the CDP model is the best fit for describing the inelastic behaviour of concrete. This model can be utilised in both ABAQUS/Standard and ABAQUS/Explicit, and the results can be transferred between the two. It is suitable for usage under all load conditions, including static and dynamic loadings. Furthermore, the CDP model posits that tensile cracking and compressive crushing are the two fundamental failure modes in concrete. In this study, the CDP model was used to analyse concrete behaviour.

### 2.1.1. Concrete Damage Plasticity Model

First, to predict the concrete's uni-axial stress-strain curve (both in compression and tension), the methodology proposed by Alfrah et al. [23] was used in this study. In Figure 3, $\sigma_{cu}$ and $\sigma_{to}$ represent compressive and tensile strengths, where as $\varepsilon_{cm}$ and $\varepsilon_{tm}$ represent the corresponding strains. According to model code 2010 [24], it is assumed that $\varepsilon_{cm} = 0.0022$, $\sigma_{cu} = \sigma_{ck} + 8$ ($\sigma_{ck}$ is the characteristic value of concrete compressive strength), and $\sigma_{to} = 0.3016 f_{ck}^{2/3}$; these stresses and the deformation modulus are stated in MPa. In Figure 3, $\bar{\varepsilon}_c^{in}$ and $\bar{\varepsilon}_{oc}^{el}$ represent the crushing and elastic undamaged strain components, while $\bar{\varepsilon}_c^{pl}$ and $\bar{\varepsilon}_c^{el}$ represent the plastic and elastic damaged strain components, respectively. $\bar{\varepsilon}_t^{ck}$ and $\bar{\varepsilon}_{ot}^{el}$ are the cracking and elastic undamaged strain components in Figure 4, while $\bar{\varepsilon}_t^{pl}$ and $\bar{\varepsilon}_t^{el}$ are the plastic and elastic damaged strain components.

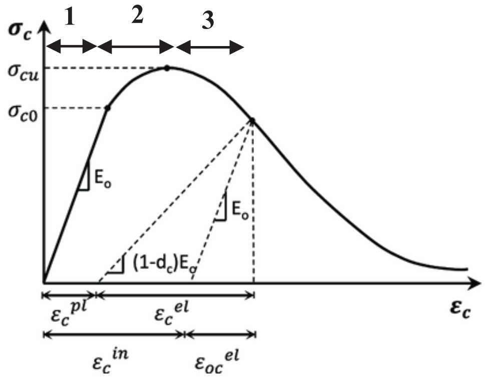


**Figure 3 - Compressive Behaviour of Concrete(Abaqus User Manual 6.14** [25]**)**

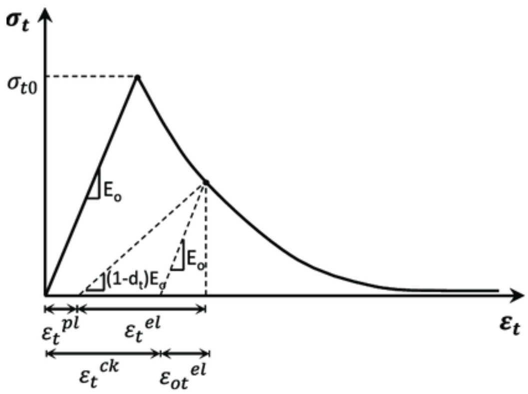


**Figure 4 – Tensile Behaviour of Concrete (Abaqus User Manual 6.14** [25]**)**

The compressive behaviour of the concrete can be divided into three segments as shown in Figure 3. The first segment is linear, $\sigma_{c(1)} = E_0 \varepsilon_c$, reaching $0.4\sigma_{cu}$. Then the second segment shows quartic behaviour between stress levels of $0.4\sigma_{cu}$ to $\sigma_{cu}$ as mentioned in Eq. (1). In Eq. (1), $E_{ci}$ is the modulus of deformation of concrete for zero stress, given by $E_{ci} = 10000\,\sigma_{cu}^{1/3}$ and $E_0 = (0.8 + 0.2\sigma_{cu}/88)$, $E_{ci}$ (in MPa). In the initial linear branch, $E_o$ is the secant modulus that corresponds to $0.4\, f_{cm}$ stress.

$$\sigma_{c(2)} = \frac{E_{ci}\frac{\varepsilon_c}{\sigma_{cu}} - \left(\frac{\varepsilon_c}{\varepsilon_{cm}}\right)^2}{1 + \left(E\frac{\varepsilon_{cm}}{\sigma_{cu}}\right)\frac{\varepsilon_c}{\varepsilon_{cm}}}\sigma_{cu} \qquad \ldots(1)$$

The third descending segment of the curve is given by Eq. (2). In Eqs. (2) and (3), $G_{ch}$ is the crushing energy per unit area and $l_{eq}$ is the characteristic length. Both $G_{ch}$ and $l_{eq}$ depend on the mesh size, the element type and the crack direction. Based on experimental observations, $b$ = 0.9 can be initially assumed [23].

$$\sigma_{c(3)} = \left(\frac{2 + \gamma_c\sigma_{cu}\varepsilon_{cm}}{2f_{cm}} - \gamma_c\varepsilon_c + \frac{\varepsilon_c^2\gamma_c}{2\varepsilon_{cm}}\right)^{-1} \qquad \ldots(2)$$

$$\gamma_c = \frac{\pi^2\sigma_{cu}\varepsilon_{cm}}{2\left[\frac{G_{ch}}{l_{eq}} - 0.5\sigma_{cu}\left(\varepsilon_{cm}(1-b) + b\frac{\sigma_{cu}}{E_0}\right)\right]^2};\ b = \frac{\varepsilon_c^{pl}}{\varepsilon_c^{ch}} \qquad \ldots(3)$$

Next, regarding the tensile behaviour of the concrete, the ratio between tensile stress $\sigma_t(w)$ (for crack width $w$) and maximum tensile strength $\sigma_{to}$, is given in Eq. (4). In Eq. (4), *c1* = 3, *c2* = 6.93 [40], and $w_c$ is the critical crack opening. Eq. (4) shows that $\sigma_t(0) = \sigma_{to}$ and that $\sigma_t(w_c) = 0$. Therefore, $w_c$ can be considered as the fracture crack opening.

$$\frac{\sigma_t(w)}{\sigma_{to}} = \left[1 + \left(c_1\frac{w}{w_c}\right)^3\right]e^{-c_2\frac{w}{w_c}} - \frac{w}{w_c}(1 + c_1^3)e^{-c_2} \qquad \ldots(4)$$

The concrete stress-strain relationship proposed by Alfarah et al. [23] mentioned above was used to define concrete material properties in this study. Developed stress-strain and damage models for compression and tension are shown in Figures 5 and 6, respectively. Defined parameters for the concrete damage plasticity model are shown in Table 1. Poisson's ratio of concrete was taken as 0.2.

**Table 1- Parameters Used for Concrete Damage Plasticity Model**

| Parameter | Value |
|---|---|
| Dilation angle | 13 |
| Eccentricity | 0.1 |
| $\boldsymbol{F_{bo}/F_{co}}$ | 1.16 |
| K factor | 0.666 |
| Viscosity | 0.0001 |

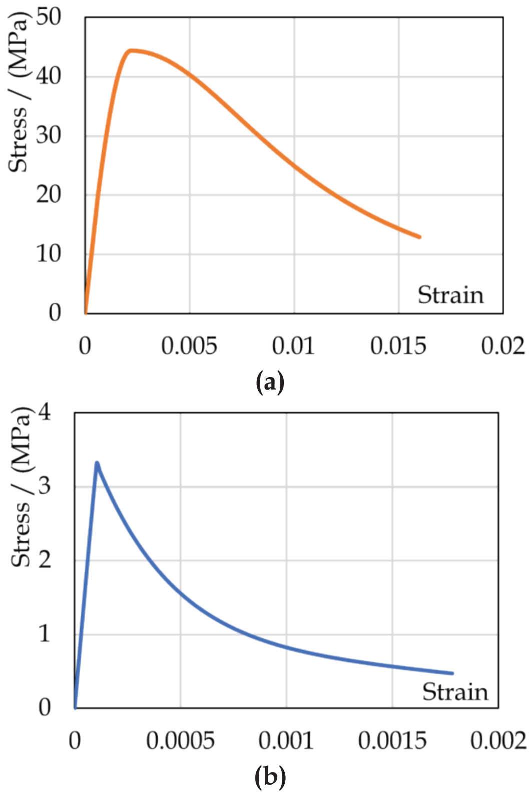


**Figure 5 - Stress-Strain Curves of Concrete: (a) Compressive Behaviour and (b) Tensile Behaviour**

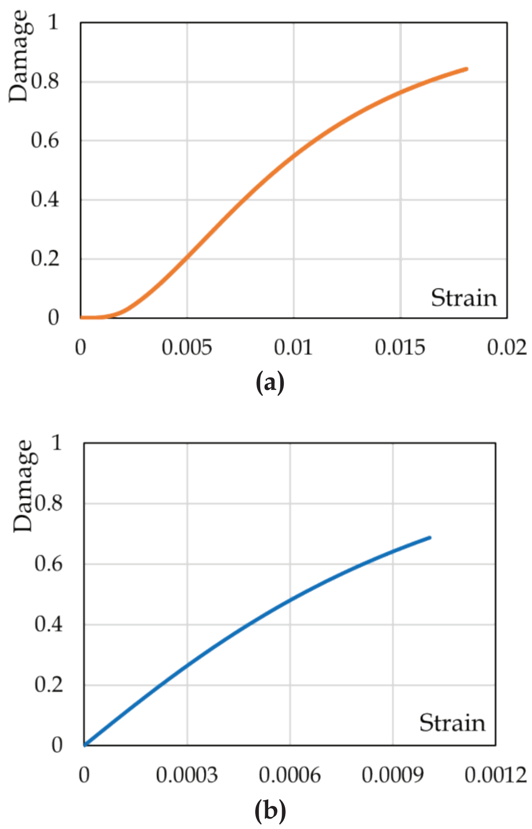


**Figure 6 - Damage-Strain Curves of Concrete:(a) Compressive and (b) Tensile Damage Behaviours**

### 2.1.2. Steel Material Properties

Steel grade and reinforcement types used in the experiment conducted by Nagaprasad et al. [26] are described below. In the specimens, high-yield strength-deformed (HYSD) steel bars (with a specified yield strength of 515 MPa) were employed for both longitudinal and transverse reinforcement. Six 16 mm diameter HYSD bars were used for longitudinal reinforcement in columns. Simultaneously, the transverse reinforcement was made out of 8 mm diameter HYSD bars spaced 100 mm apart. Similarly, 10 mm diameter HYSD bars were employed for longitudinal and transverse reinforcement in specimen footing. Each strengthened specimen consisted of hot-rolled Indian Standard sections ISA35×35×5 @ 26.0 N/m for steel angle sections and 6mm thick mild steel plates for battens. As stated above, same steel grade and reinforcement type used in the Nagapasad et al. [26] experimental setup were used in the numerical model.

Many studies modelled the elastic-plastic stress-strain relationship of steel as bilinear [2,10,13,27]. The yield criterion of the model plays a significant role in the modelling process. As we consider steel as an isotropic material, the von mises yield criterion was employed in most studies [12,28]. Three types of hardening models can be used for material modelling: Isotropic hardening, Kinematic hardening and Combined hardening. Both kinematic and combined hardening criteria were used in past studies and are compatible with the experimental results [13]. All these three material models and the Von mises criterion can be employed in ABAQUS [25].

The Young's modulus and Poison's ratio of steel were defined as 200 GPa and 0.3, respectively, and the bilinear stress-strain curve, as shown in Figure 7, was adopted for the study. In addition, the Isotropic/Kinematic (Combined) hardening property available in ABAQUS was implemented to represent increasing cyclic loading arrangement for the validation with the von-mises yield criterion as discussed above.

Further, the stress-strain behaviour of the reinforcement incorporating the hardening behaviour of the rebar is essential to predict the reliable behaviour of the RC column. True stress – True strain behaviour of the rebar was given, as shown in Figure 8.

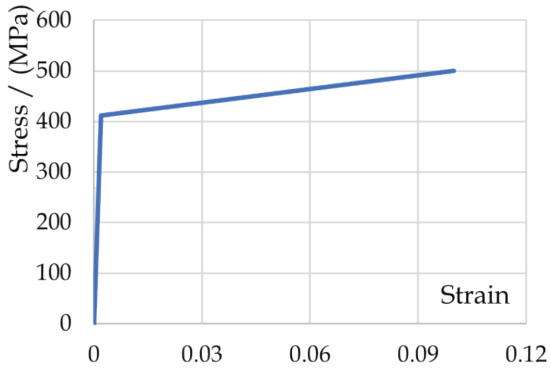


**Figure 7 - Bilinear Stress-Strain Curve of Steel**

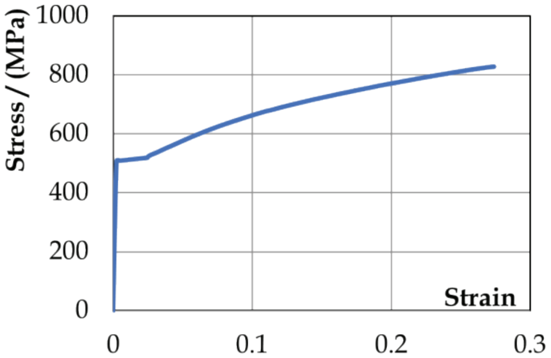


**Figure 8 - Stress-Strain Curve of Rebar**

### 2.2. Numerical Modelling

FE model of a strengthened RC column consists of concrete, steel and rebars. First, the eight-node brick elements with three translational degrees of freedom at each node (C3D8R) were used to model both concrete and steel jackets. Then the longitudinal rebars and stirrups were modelled using two node truss elements (T3D2). After that, the interaction between steel angles and concrete was modelled with the surface-to-surface connection with a tangential friction coefficient of 0.4 ($\mu = 0.4$) [11]. In addition to that, finite sliding was allowed in this model to allow arbitrary relative separation, sliding, and rotation of the contacting surfaces.

On the other hand, hard interaction (no friction) between steel jackets and concrete was provided in the normal direction to prevent concrete movement beyond steel plates. Further, rebars were embedded into the concrete to avoid slipping between them [3,27]. However, in the numerical model, binding layer between L angle and the concrete is not provided, since it is not affecting the accuracy of the model [27].

Further, all degrees of freedom are restrained at the base surface of the column rather than simulating the foundation [2,10,12]. On the other hand, the strengthened column with a foundation was used in the experiment. Under earthquake conditions, RC columns of a moment-resisting frame bend in double curvature [29,30]. As a result, the inflexion points can be considered to be at their mid-height, separating the entire column into two cantilever portions of length equal to one-half of the story height. In the experimental study [26], test specimens were taken from the base of the column to its point of inflexion. Hence, the steel jacket and the column were fixed at the bottom of this study. Only half of the column was modelled and analysed by applying symmetry boundary conditions in corresponding planes.

Finally, a convergence test was conducted to determine the suitable element size with less computational time, which was found to be 40 mm for both concrete and steel jackets.

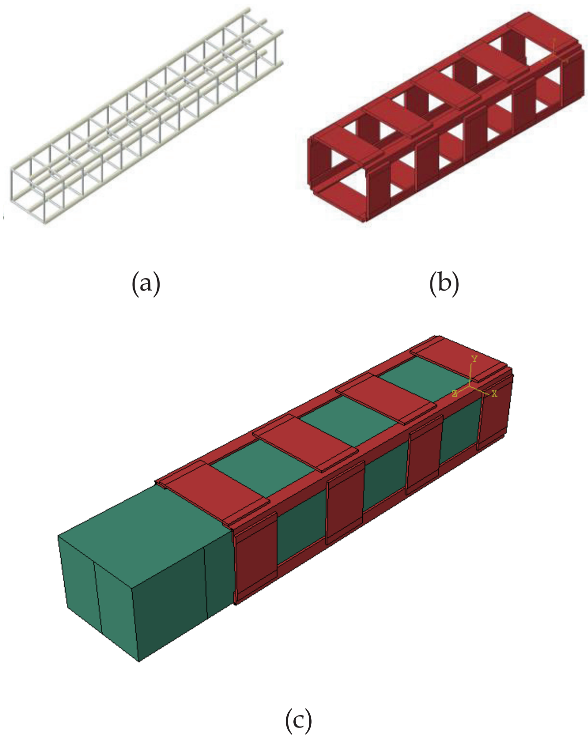


**Figure 9 - Finite Element Model: (a) Reinforcement Arrangement, (b) Steel Jacket and (c) Whole Model**

### 2.3. Loading Sequence

Initially, for the FE model validation, the specimen was loaded with a 450 kN axial load (as a uniformly distributed pressure load) along with the lateral cyclic loading at the top of the specimen (See Figure 10). Afterwards, the parametric study was conducted using a 150 mm linearly increasing lateral load along with the same axial load given to the validated model.

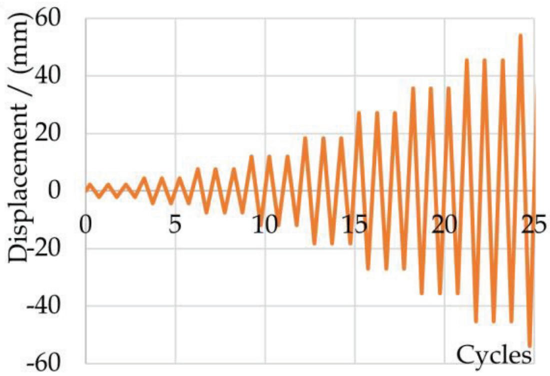


**Figure 10 - Fully Reversed Loading for Validation** [26]

**2.4. Specimen Geometry**

The study was conducted in two stages: (1) analysing previous test specimens under increasing fully reversed cyclic load to validate the model, (2) conducting a parametric study using increasing lateral load. First, the developed numerical model was intended to be validated using the experimental results by Pasala Nagaprasad et al. [26]. So, the finite element model was developed exactly the same as the tested column, where the column and foundation dimensions used in the test are 200x250x1275 mm and 900x720x400 mm (See Figure 10). For both the longitudinal and transverse reinforcement of each specimen, high-yield strength-deformed (HYSD) steel bars were utilised, with the yield strength specified as being 415 MPa. The transverse reinforcement in columns was made up of 8 mm diameter HYSD bars at a centre-to-centre spacing of 100 mm, while the longitudinal reinforcement in columns was made up of six numbers of 16 mm diameter HYSD bars. Similar to this, HYSD bars with a 10 mm diameter were employed for specimen footing reinforcement in both the longitudinal and transverse directions. Further, the steel jacket's dimensions are batten width=80, batten spacing=225 mm, batten thickness=6 mm and L angle thickness =6 mm (see Figure 11). In addition, a comparison between column performance with and without footing was also conducted to reduce the computational time without affecting the accuracy.

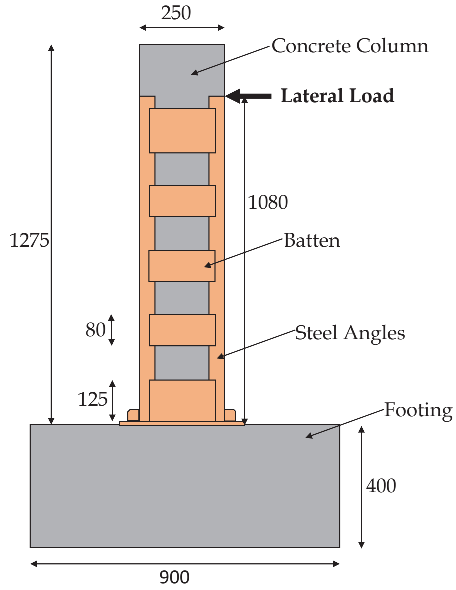


**Figure 11 - Experimental Test Setup of Nagaprasadet al.** [26] **(All Dimensions are in mm)**

In the second step, effect of each steel jacket parameters (see Figure 12 and Table 2) can be evaluated through the extensive parametric study using FE models. It is, therefore, possible to carry out a parametric study with validated FE models following the specimen geometries stated previously. This parametric study provides more extensive information on the behaviour of an RC column strengthened with a steel jacket, as well as the parameters that influence this behaviour. By modelling the failure of each specimen, the ultimate load obtained from each model can be compared to the ultimate load obtained from the base model. Table 2 summarises the dimensions of the specimens examined in the parametric investigation.

Each specimen set represents the following special features:

(a). Standard specimen: This specimen's parameters are the standard of comparison for the influence of variations in each analysed parameter. The steel jacket's geometry is slightly modified compared to the test specimen. Specifically, the height of the column was reduced from 1080 mm to 1000 mm, and the batten width was increased from 80 mm to 83 mm. These modifications were made to enable a more comprehensive study of the behaviour of the connection under different loading conditions.

**Table 2 – Specimen Geometries for Parametric Study**

| Specimen | Batten Spacing / (mm) | Batten Width / (mm) | Jacket Height / (mm) | L angle Thickness / (mm) | Batten Thickness / (mm) |
|---|---|---|---|---|---|
| Standard | 225 | 100 | 1000 | 6 | 6 |
| BS-150 | 150 | 100 | 1000 | 6 | 6 |
| BS-300 | 300 | 100 | 1000 | 6 | 6 |
| BW-83 | 225 | 83 | 1000 | 6 | 6 |
| BW-125 | 225 | 125 | 1000 | 6 | 6 |
| EBW-125 | 225 | 100 | 1000 | 6 | 6 |
| EBW-150 | 225 | 100 | 1000 | 6 | 6 |
| EBW-175 | 225 | 100 | 1000 | 6 | 6 |
| EBW-200 | 225 | 100 | 1000 | 6 | 6 |
| H-100 | 225 | 100 | 100 | 6 | 6 |
| H-325 | 225 | 100 | 325 | 6 | 6 |
| H-550 | 225 | 100 | 550 | 6 | 6 |
| H-775 | 225 | 100 | 775 | 6 | 6 |
| BT-9 | 225 | 100 | 1000 | 6 | 9 |
| BT-12 | 225 | 100 | 1000 | 6 | 12 |
| LT-9 | 225 | 100 | 1000 | 9 | 6 |
| LT-12 | 225 | 100 | 1000 | 12 | 6 |

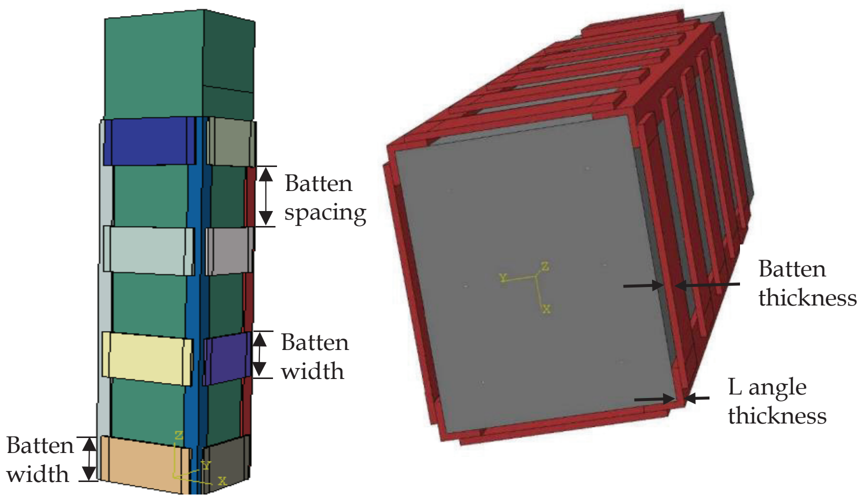


**Figure 12 - Steel Jackets' Parameters included in the Parametric Study**

(b). Specimens BS-150 and BS-300: The sole variation between these specimens and the standard specimen is the batten spacing of the cage, where the BS stands for batten spacing and the numbers represent batten spacing (150 mm and 300 mm). This provides a basis for investigating the effect of batten spacing on the behaviour of the strengthened column.

(c). Specimens BW-83 and BW-125: The only difference between these specimens and the standard specimen is in the batten width of the cage, where the BW indicates batten width and the numbers indicate the width of the batten (83 mm and 125 mm).

(d). Critical area in terms of the behaviour of the strengthened column is at the ends of the column. Specimens EBW-125, EBW-150, EBW-175 and EBW-200 are used to understand the performance of the column. The only difference between these and standard specimens is the jacket's end batten width (EBW). The end batten widths are 125, 150, 175 and 200 mm.

(e). Specimens H-100, H-325, H-550 and H-775. These specimens are studied to determine the influence of the steel jacket height (H) on the behaviour of the strengthened column.

(f). Specimens BT-9, BT-12 and LT-9, LT-12 are used to understand the effect of batten thickness (BT) and L angle thickness (LT) on the performance of the strengthened column.

## 3. Results and Discussion

### 3.1. Validation of the Finite Element Model

The FE model's hysteretic and envelop curves were compared to experimental results reported in the literature [7]. The combined hardening model predicted the experimental results quite well (see Figure 13).

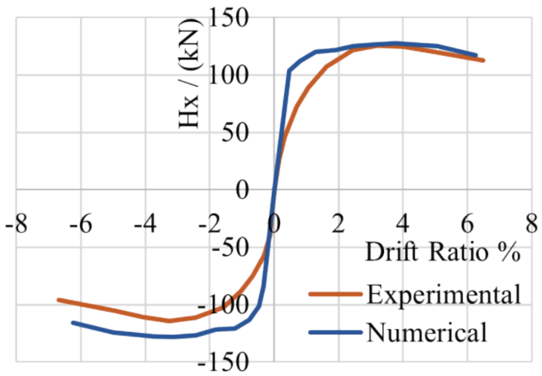


**Figure 13 - Comparison Between Experimental and Numerical Results**

The combined hardening model, on the other hand, is a combination of isotropic and kinematic hardening in which the yield surface extends symmetrically and moves in the stress space [28]. Lateral strength at any displacement level was determined by averaging peak lateral resistance in both directions of cyclic excursion. As shown in Figure 13, the numerical backbone curve agrees with the experimental curve, where positive curves after the peak load are almost identical. The pinching effect of the RC column under cyclic loading cannot be reflected in ABAQUS concrete damage plasticity model [10]. After the first loading, due to the tension at the rear face of the column, the stiffness of the column is reduced for reversal loading. Hence the experimental values are lesser than the numerical values in the reversal branch. However, the experimental and numerical results were almost identical, so the developed model was used for the parametric study.

### 3.2. Effects of Design Parameters on the Performance of the Strengthened Column

As the first step of the parametric study, the strengthened column was modelled with and without footing to compare the analytical accuracy of the FE model. As shown in Figure 14, the deviation in envelop curves between the model with and without foundation was negligible. So, the fixed support boundary condition instead of footing adequately represents the foundation of the columns.

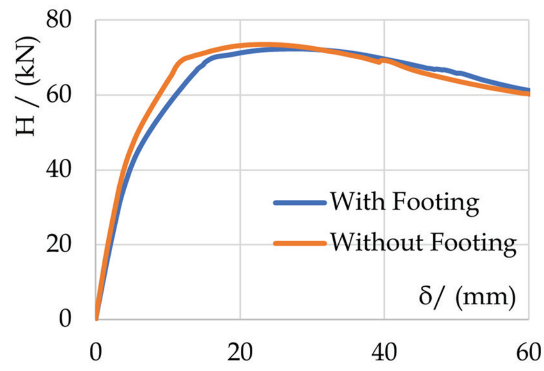


**Figure 14 - Comparison of Lateral Load-Displacement Curves Between the Model with Footing and without Footing**

#### 3.2.1. Batten spacing and Batten Width

The batten spacing of the standard column is 225 mm, and the parametric study has been performed for models with batten spacing of 150 mm, 225 mm, 300 mm and unstrengthen column. The comparison of lateral loading curves is shown in Figure 15. The lateral strength of the models with batten spacing of 300 mm, 225 mm, and 150 mm are 132.77 kN, 134.06 kN and 137.35 kN, respectively. As illustrated in Figure 15, maximum strength increased by 101%, 103% and 108% with increasing batten spacing compared to the strengthened model.

In the BS series, the number of battens positively influenced failure load; lowering batten spacing from 300 mm to 150 mm improved failure loads by 115%. This is due to the batten's continuity throughout the specimen height, which protected the specimen from spalling by increasing confinement, particularly at the bottom of the column. Further, a comparable increment in ultimate displacement was observed with the decreasing batten spacing. For example, ultimate displacement has increased by 4.24% and 8.62%, respectively, for 225 mm and 150 mm batten spacing, compared to the 300 mm. It can be observed from Figure 15 that the strength distortion rate after the maximum load also decreased in the strengthened column. Further, with the decreasing batten spacing, the distortion rate also reduced significantly in the specimen with a spacing of 150 mm.

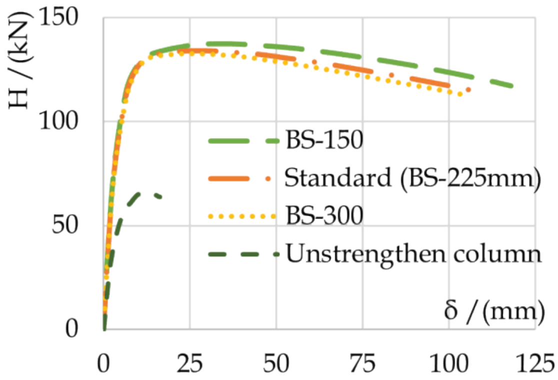


**Figure 15 - Lateral Loading Curves for Each Batten Spacing**

As illustrated in Figure 16, the batten width was changed to 83 mm, 100 mm and 125 mm without changing the total cross-sectional area of the battens. The resultant lateral capacities are 133.46 kN, 134.06 kN and 135.46 kN, respectively. However, as shown in Figure 16, a significant improvement could not be observed in lateral strength, yield strength, or ultimate displacement. Even though, all the strengthened columns with different batten space showed almost 105%, and 150% increments in both ultimate strength and displacement, respectively.

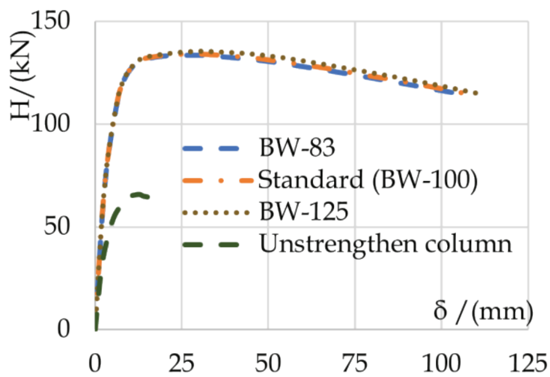


**Figure 16 - Lateral Loading Curves for Each Batten Width**

However, batten width has an insignificant effect on strength and ductility. This confirms that the primary factor in achieving improved strength and ductility is the use of steel jacketing to provide lateral confinement to the column. Therefore, while adjusting the batten width may affect the distribution of the lateral confining pressure on the column, the design of the steel jacket should prioritize achieving the required amount of lateral confinement, as this is the key factor in improving the overall performance of the column.

### 3.2.2. End Batten Width

The width of the batten at the bottom of the column was changed from 100 mm to 200 mm to study the effect of end batten width on the performance. As shown in Figure 17, the lateral strength of the system increased with the increasing end batten width. The maximum lateral strengths are 134.06 kN, 136.09 kN, 139.71 kN, 144.37 kN and 150.9 kN for end batten widths of 100 mm, 125 mm, 150 mm, 175 mm and 200 mm, respectively. Further, the increment of lateral strength compared to the strengthened model is 109% to 140% by increasing the end batten width from 100 mm to 200 mm, respectively. This observation further strengthens that the increase in the area of the batten increases the strength of the column due to the increased confinement. Especially, the failure of the column observed in the ends, and increasing the width of the batten at the end can be utilised to postpone the failure of the column. Further, this observation shows another possibility to increase the strengthened column's strength by adding more battens at the end. In addition, yield strength and ultimate displacement have also increased by increasing the end batten width. A total 300% increment of ultimate displacement was achieved in the model with a 200 mm end batten width compared to the strengthened model.

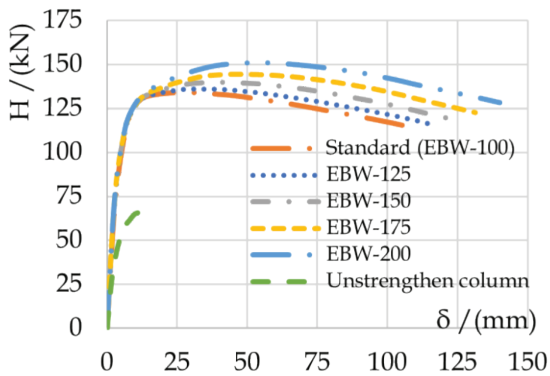


**Figure 17 - Lateral Loading Curves for Each End Batten Width**

### 3.2.3. Height of the Steel Jacket

In order to determine the effect of steel jacket height on the lateral performance, the height of the steel jacket was changed, keeping all other dimensions of the jacket (base model) unchanged. Height was changed to 100 mm, 325 mm, 550 mm, 775 mm and 1000 mm. As shown in Figure18, maximum lateral capacities were found as 90.26 kN, 115.46 kN, 131.9 kN, 133.19 kN and 134.06 kN respectively, which are respectively 36.9%, 75%, 100%, 102.8% and 103% larger than unstrengthen column.

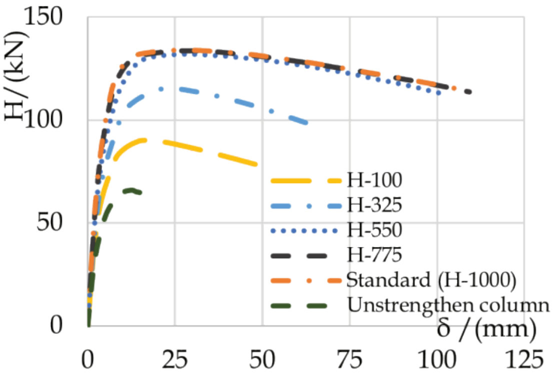


**Figure 18 - Lateral Loading Curves for Each Steel Jacket Height**

Even though the strength and ductility increase with the increasing steel jacket height, after 550 mm height, considerable improvement has not been achieved by increasing the jacket height. This observation indicates that providing steel jackets up to the 1/3rd of the column is adequate to enhance the lateral performance and providing more than that height is ineffective too. Furthermore, as shown in Figure 18, yield strengths and ductility have improved similarly. The encased steel deformation does not increase with the steel jacket height, and there is minor deformation in the upper part of the cased steel with a jacket height of 775 mm, as shown in Figure 21.

Stress distribution in steel jackets and the variation of compressive damage with the steel jacket height are shown in Figure 21. As shown in Figure 21, with the steel jacket height, the spread of compressive damage in concrete is reduced. In addition to the small difference in compressive damage between H-775, H-1000 indicates that providing a steel jacket up to a certain height is more than enough to enhance the lateral performance of the strengthened column.

### 3.2.4. Batten Thickness

The initial value of the batten thickness was 6 mm in the basic model and increased up to 9 mm and 12 mm to investigate the effect on the lateral performance. The achieved maximum lateral strengths are 134.06 kN, 135.5 kN and 137.8 kN, respectively. It shows an increase in lateral strengths from 1.1% and 1.68% compared to the basic model (6 mm). Whereas the yield strength has not increased for the 9 mm model, the 12 mm model shows a 3.99% increment compared to the other two models. As shown in Figure 19, considerable improvement has not been achieved for ultimate displacement by increasing the batten thickness.

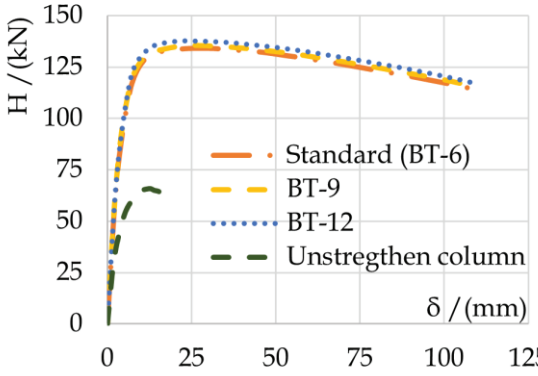


**Figure 19 - Lateral Loading Curves for Each Batten Thickness**

### 3.2.5. L angle Thickness

Numerical Analysis was performed for the models with L Angle with different thicknesses of 6 mm, 9 mm and 12 mm. The lateral capacities have increased drastically with the increasing L angle thickness. As shown in Figure 20, resultant maximum lateral strength values are 134.06 kN, 154.6 kN and 170.7 kN, respectively, which are 103%, 135% and 159% higher than the un strengthened column. On the other hand, improvement in yield strength was also observed, such as 131.17 kN and 140.2 kN for the L angle thicknesses of 9 mm and 12 mm, respectively, where percentage increments are 15.32% and 19.41% compared to the 6 mm thickness. The improvement of ultimate displacement from 6 mm to 12 mm is more than 34%. Hence increasing the L angle thickness yields to large improvement in both strength and displacement.

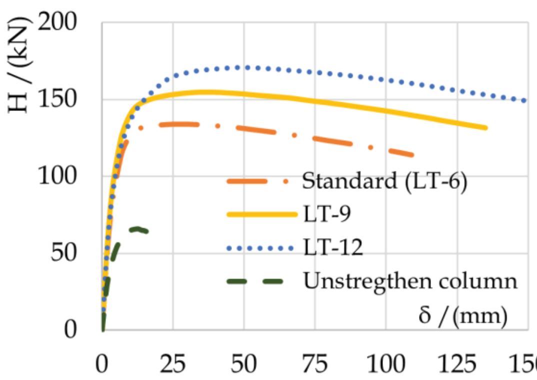


**Figure 20 - Lateral Loading Curves for Each L Angle Thickness**

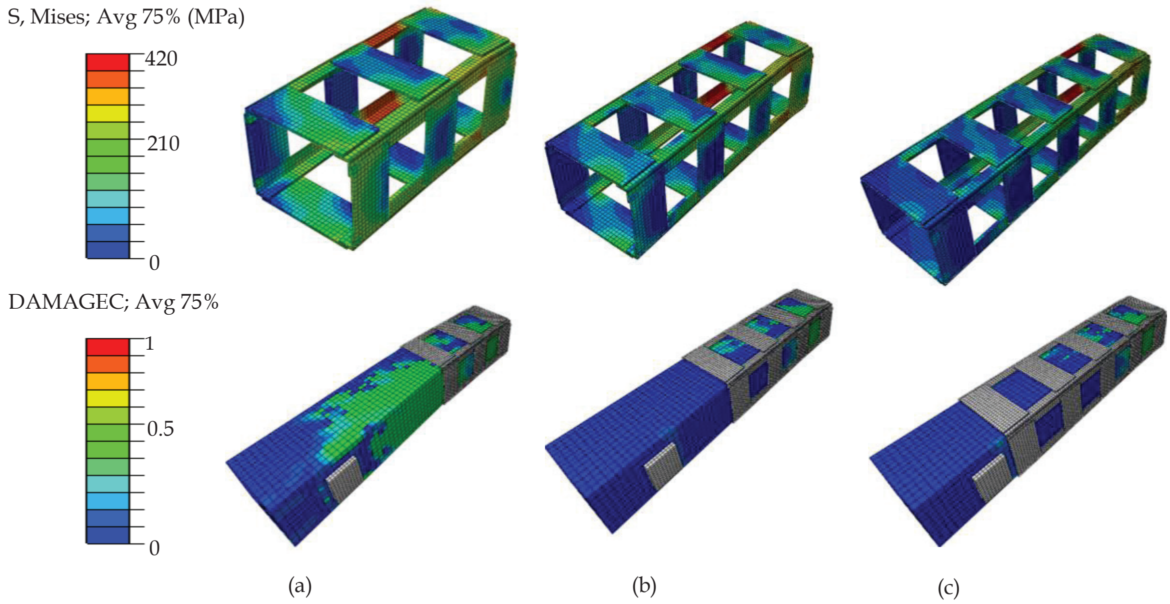


**Figure 21 – Stress Variation and Compressive Damage of Steel Jackets and RC Column with Steel Jacket Height: (a) H-550, (b) H-775 and (c) Standard Column (H-1000)**

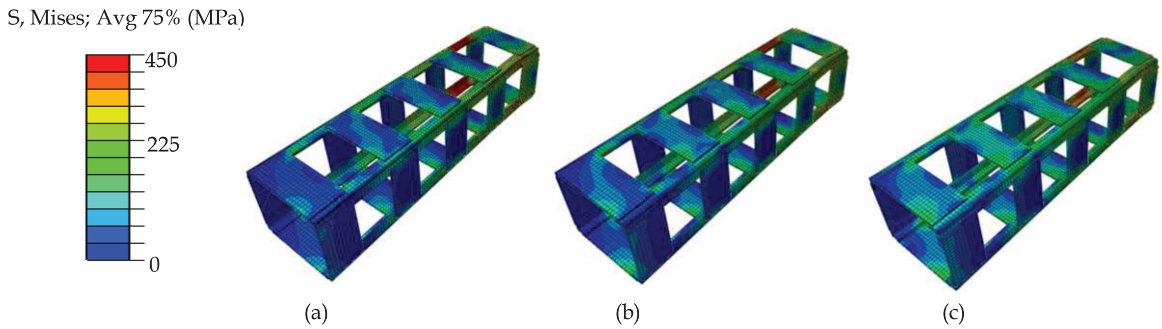


**Figure 22 – Stress Distribution Along the Steel Jackets with the L Angle Thickness: (a) LT-6, (b) LT-9 and (c) LT-12**

Increasing the L-angle thickness can effectively postpone the yielding of the angles at the bottom of the column, Figure 22. As shown in Figure 22, in all the cases, bottom L angles reach the yield stress first, so by postponing the yielding of the angle by increasing the thickness effectively helps to increase the strength and ductility of the system.

## 4. Conclusion

The steel jacketing technique can be used to enhance the seismic performance of the columns. The steel jacketing method using four L-angles welded with horizontal battens was studied using numerical simulations under lateral loading conditions. A parametric study was performed to investigate the behaviour of each parameter of the steel jacket, such as the cross-sectional area of the horizontal battens, the height of the steel jacket, the thickness of the battens and the steel angles. The technique's performance was studied by comparing three critical parameters, lateral capacity, yield strength and ductility. Based on the study, conclusions are as follows;

1. The steel jacketing method mentioned in the study significantly improves the lateral/seismic strength of the RC column by more than 100% and is simultaneously an effective method to enhance the yield strength and the ductility of the column.

2. The performance of the steel jacket depends on the cross-sectional area of the horizontal battens/plates rather than its width. Therefore, reducing the batten spacing has a better impact on improving ductility than lateral strength, hence can be used on

occasion when the ductility of a column needs to be increased.

3. The batten spacing has a significant impact on the load-carrying capability of an RC reinforced column. Closely spaced strips can substantially constrain the concrete, preventing it from expanding laterally when subjected to compressive and lateral forces.
4. Increasing the height of the steel jacket is an excellent option to increase the lateral strength, yield strength and ductility but the effectiveness is up to 1/3rd of the RC column height.
5. The steel cage's end batten is located in the RC column's probable plastic hinge zone, which has a significant impact on its overall behavior under lateral pressures. The jacketed column also failed at the bottom of the steel angles. As a result of the greater confinement effect, extending the width of end battens in the projected plastic hinge zone of the steel cage effectively increases the compressive strength of concrete and reduces the possibility of local buckling of steel angles.
6. Even though the slight improvement in lateral strength and yield strength can be achieved by increasing the batten thickness, improvement in ductility could not be achieved. Hence increasing the batten thickness is not a practical option to enhance the performance of the jacket system.
7. Increasing the thickness of the L-angles can be identified as the best option to enhance the lateral performance of the steel-jacketed column as it has achieved 159% improvement in strength compared to the unstrengthen model by increasing the L-angle thickness from 6mm to 12 mm. Further, by doubling the L-angle thickness from 6mm, almost 25%, 19% and 34% improvement can be gained in lateral strength, yield strength and ductility, respectively.

## References


1. Siddika, A., Al Mamun, M. A., Ferdous, W., Alyousef, R., Performances, Challenges and Opportunities in Strengthening Reinforced Concrete Structures by using FRPs – A State-of-the-Art Review, Eng. Fail. Anal. 111 (2020) 104480. https://doi.org/10.1016/j.engfailanal.2020.104480.
2. Belal, M. F., Mohamed, H. M., Morad, S. A., Behavior of Reinforced Concrete Columns Strengthened by Steel Jacket, HBRC J. 11 (2015) 201–212. https://doi.org/10.1016/j.hbrcj.2014.05.002.
3. Matias, J. V., Júlio, E., Silvestre, N., Numerical Modelling of Circular Concrete Columns Strengthened with Hybrid frp Jackets, (n.d.) 1–11.
4. Li, J., Gong, J., Wang, L., Seismic Behavior of Corrosion-Damaged Reinforced Concrete Columns Strengthened using Combined Carbon Fiber-Reinforced Polymer and Steel Jacket, Constr. Build.(2009) 2653–2663. https://doi.org/10.1016/j.conbuildmat.2009.01.003.
5. Villar-Salinas, S., Guzmán, A., Carrillo, J., Performance Evaluation of Structures with Reinforced Concrete Columns Retrofitted with Steel Jacketing, J. Build. Eng. 33 (2021) 101510. https://doi.org/10.1016/j.jobe.2020.101510.
6. Pohoryles, D.A., Rossetto, T., Numerical Modelling of frp-Strengthened RC Beam-, (2015) 1–10.
7. Nagaprasad, P., Sahoo, D. R., Rai, D. C., Seismic Strengthening of RC Columns using External Steel Cage, Pacific Conf. Earthq. Eng. (2007) 1–6. https://doi.org/10.1002/eqe.
8. E.T.D.E.S. De, S. Charges, A. Et, Behavior of Slender Concrete Columns Reinforced with gfrp-Bars and Spirals, (2020) 1–12.
9. Zeng, J., Guo, Y., Li, L., Chen, W., Behavior and Three-Dimensional Finite Element Modeling of Circular Concrete Columns Partially Wrapped with FRP Strips, Polymers (Basel). 10 (2018). https://doi.org/10.3390/polym10030253.
10. Xu, C. X., Peng, S., Deng, J., Wan, C., Study on Seismic Behavior of Encased Steel Jacket-Strengthened Earthquake-Damaged Composite Steel-Concrete Columns, J. Build. Eng. 17 (2018) 154–166. https://doi.org/10.1016/j.jobe.2018.02.010.
11. Júlio, E.N.B.S., Branco, F.A.B., Reinforced Concrete Jacketing - Interface Influence on Cyclic Loading Response, ACI Struct. J. 105 (2008)471–477. https://doi.org/10.14359/19861.
12. Adam, J. M., Ivorra, S., Pallarés, F.J., Giménez, E., Calderón, P.A., Axially Loaded RC Columns Strengthened by Steel Caging. Finite Element Modelling, Constr. Build.(2009)2265–2276.

https://doi.org/10.1016/j.conbuildmat.2008.11.014.

13. Mahdavi, N., Tasnimi, A. A., Modeling and Verification of Response of RC Columns Strengthened in Flexure with Mechanically Fastened FRP, J. Vibroengineering. 20 (2018) 1774–1782. https://doi.org/10.21595/jve.2018.18990.

14. Islam, N., Hoque, M. M., Strengthening of Reinforced Concrete Columns by Steel Jacketing: A State of Review, Asian Trans. Eng. 5 (2015) 6–14.

15. Naji, A.J., Al-Jelawy, H.M., Saadoon, S.A., Ejel, A.T., Rehabilitation and Strengthening Techniques for Reinforced Concrete Columns: Review, J. Phys. Conf. Ser. 1895 (2021). https://doi.org/10.1088/1742-6596/1895/1/012049.

16. Brena, S.F., A. Sergio M, Seismic Performance Evaluation of Rehabilitated Reinforced Concrete Columns through Jacketing, Improv. Seism. Perform. Exist. Build. Other Struct. - Proc. 2009 ATC SEI Conf. Improv. Seism. Perform. Exist. Build. Other Struct. (2009) 572–583.

17. Elsamny, M.K., Hussein, A.A., Nafie, A.M., Abd-Elhamed, M.K., Experimental Study of Eccentrically Loaded Columns\Strengthened using a steel Jacketing Technique, 7 (2013) 1–8.

18. Brena, S.F., Alcocer, S.M., Seismic Performance Evaluation of Rehabilitated Reinforced Concrete Columns through Jacketing, Improv. Seism. Perform. Exist. Build. Other Struct. - Proc. 2009 ATC SEI Conf. Improv. Seism. Perform. Exist. Build. Other Struct. (2009) 572–583.

19. Jenothan, M., Jayasinghe, J.A.S.C., Bandara, C.S., Lateral Behaviour and Performance Evaluation of Steel Piers under Cyclic Latera Loading, J. Constr. Steel Res. 201 (2023) 107764. https://doi.org/10.1016/j.jcsr.2022.107764.

20. Jenothan, M., Yuvahini, V., Bandara, C.S., Jayasinghe, J.A.S.C., Experimental and Numerical Study on Force – Displacement & Moment – Curvature Behaviour of a Reinforced Concrete Beam, (n.d.) 1–7.

21. Sinaei, H., Evaluation of Reinforced Concrete Beam Behaviour using Finite Element Analysis by ABAQUS, Sci. Res. Essays. 7 (2012) 2002–2009. https://doi.org/10.5897/sre11.1393.

22. Sethuraman, V.S., Suguna, K., Raghunath, P.N., Numerical Analysis of High Strength Concrete with Cyclic Loading using Abaqus, Glob. J. Pure Appl. Math. 13 (2017) 225–235. http://www.ripublication.com.

23. B. Alfarah, F. López-Almansa, S. Oller, New methodology for calculating damage variables evolution in plastic damage model for RC structures, Eng. Struct. 132 (2017) 70–86. https://doi.org/10.1016/j.engstruct.2016.11.022.

24. CEB-FIP, CEBFIP, Model code 2010, Euro-International Du Bet. 594 (2010).

25. ABAQUS, Abaqus 6.14, Abaqus 6.14 Anal. User's Guid. (2014) 14.

26. Nagaprasad,P., Sahoo, D.R., Rai, D.C., Seismic Strengthening of RC columns using external steel cage, Earthq. Eng. Struct. Dyn. (2009) 1–6. https://doi.org/10.1002/eqe.

27. De Almeida I.,, Carvalho V., Numerical Modelling of the Behavior of Concrete Columns Strengthened by Jacketing, Inst. Super. Técnico, Univ. Lisboa. (2011) 1–12.

28. Jenothan, M., Jayasinghe, J.A.S.C., Bandara, C.S., A.J. Dammika, Lateral Performance of Thin-Walled Steel Box Column with Replaceable Energy Dissipation Mechanism, (2023) 201–214. https://doi.org/10.1007/978-981-19-2886-4_15.

29. Akino, K., Mochizuki, K., Seismic Design and Development., Proc. - IEEE Reg. 6 Conf. (1979) 279–293.

30. Pan, A., Reinforced Concrete Structures, Princ. Struct. Des. (2005) 1–48. https://doi.org/10.1201/9781420037135.ch4.